MR Imaging of Laryngeal and Hypopharyngeal Cancer

Minerva Becker, MD[a,*], Yann Monnier, MD, PhD[b], Claudio de Vito, MD, PhD[c]

KEYWORDS

• MR imaging • Diffusion-weighted imaging • Larynx and hypopharynx • Head and neck cancer

KEY POINTS

- State-of-the-art MR imaging of the larynx and hypopharynx with high-resolution morphologic and DWI sequences has an increased precision for tumor delineation than CT, thereby facilitating tailored treatment with the ultimate goal to improve patient care.
- Current diagnostic MR imaging criteria combining DWI features with distinct signal intensity patterns on morphologic sequences allow improved discrimination between tumor, peritumoral inflammation, and fibrosis.
- Multiparametric MR imaging is particularly useful for the assessment of paraglottic space invasion, for the characterization of laryngeal cartilage abnormalities, and for the detection of extralaryngeal tumor spread, all of which can be misinterpreted on CT scans.
- DWI MR imaging has a higher diagnostic performance than CT for the detection and precise depiction of post-treatment residual and recurrent disease in the larynx and hypopharynx.

INTRODUCTION

Laryngeal cancer represents about 1% to 2% of cancers worldwide and, although the incidence is decreasing in some countries, the global incidence is increasing.[1] The highest incidence is seen in Europe followed by the Americas, whereas the ratio between death and incidence is highest in Africa.[1] The worldwide incidence of hypopharyngeal cancer is about 0.5% to 1% with a well-documented increasing incidence in women in several countries.[2,3] Over 95% of laryngeal and hypopharyngeal cancers are squamous cell carcinomas (SCCs) caused mainly by tobacco and alcohol consumption and, in contrast to oropharyngeal cancer, infection with the human papillomavirus does not play an important role.[4]

During the past 20 years, the work-up of patients with suspected cancer of the larynx and hypopharynx has been primarily done with endoscopic biopsy for the assessment of mucosal abnormalities and with multislice computed tomography (CT) for the detection of submucosal tumor spread, the complementarity of both diagnostic tools requiring a close, multidisciplinary cooperation.[5–7] This combined information allows tumors to be classified according to AJCC/UICC guidelines[8,9] and therapeutic decisions to be made. However, MR imaging is increasingly regarded in many institutions as the method of choice not only for precise localization of laryngeal and hypopharyngeal cancer but also for accurate assessment of key anatomic subsites. Advantages of MR imaging in comparison to CT include a

[a] Diagnostic Department, Division of Radiology, Unit of Head and Neck and Maxillo-facial Radiology, Geneva University Hospitals, University of Geneva, Rue Gabrielle-Perret-Gentil 4, Geneva 14, Geneva 1211, Switzerland; [b] Department of Clinical Neurosciences, Clinic of Otorhinolaryngology, Head and Neck Surgery, Unit of Cervicofacial Surgery, Geneva University Hospitals, Rue Gabrielle-Perret-Gentil 4, Geneva 14, Geneva 1211, Switzerland; [c] Diagnostic Department, Division of Clinical Pathology, Geneva University Hospitals, Rue Gabrielle-Perret-Gentil 4, Geneva 14, Geneva 1211, Switzerland
* Corresponding author.
E-mail address: Minerva.Becker@hcuge.ch

Magn Reson Imaging Clin N Am 30 (2022) 53–72
https://doi.org/10.1016/j.mric.2021.08.002

superior soft-tissue contrast enabling the detection of subtle soft-tissue abnormalities, an increased discrimination capability between tumor and peritumoral inflammatory changes, improved assessment of laryngeal cartilage abnormalities, improved tumor delineation for highly focused radiotherapy and transoral laser microsurgery, and a higher diagnostic performance for the detection and precise depiction of post-treatment residual or recurrent disease.[7,10–19] However, some relative drawbacks of MR imaging in comparison to CT persist, including a longer acquisition time and motion artifacts requiring improved patient cooperation, a lower spatial resolution, and technical challenges related to air-tissue interfaces affecting image quality of diffusion-weighted imaging (DWI) sequences.

This review discusses the current state-of-the-art MR imaging examination protocols for oncologic imaging of the larynx and hypopharynx, key anatomic areas, and characteristic imaging features of laryngeal and hypopharyngeal tumors focusing on clinically relevant information in SCC and it equally addresses potential pitfalls of image interpretation. Correlation with endoscopic and histopathologic features is provided to highlight key concepts and imaging pearls.

IMAGING TECHNIQUE AND PROTOCOLS

One of the key issues when imaging laryngeal and hypopharyngeal cancer is spatial resolution, which is crucial for accurate tumor evaluation. For routine MR imaging, most authors advocate the use of either 1.5T or 3T scanners, the latter providing a higher signal-to-noise ratio, which is preferable if thinner slices are used for imaging. The coils routinely used to image laryngeal and hypopharyngeal cancers include dedicated head and neck phased array coils (groups of overlapping coils linked to a common output), parallel imaging array coils (groups of coils with a high level of decoupling optimized for artifact-free parallel imaging performance), or local circular receive surface coils placed around the larynx.[11–13,20–23] Local circular surface coils can be used alone or they can be combined with head coils. They have a small field of view and an increased signal-to-noise ratio for tissues adjacent to the loop, hence, slice thickness and in-plane resolution can be substantially improved. Nevertheless, the area covered is restricted allowing imaging of the larynx/hypopharynx only. In addition, the placement of loop surface coils around the larynx can be challenging and requires precise positioning by an experienced technician. Incorrect coil positioning can result in a reduced signal to noise, limited penetration depth, signal void in the anterior larynx, or fold-back artifacts.[24] As the circular surface coils need to be positioned relatively tightly on the patient's neck, the uncomfortable position can further lead to motion artifacts during image acquisition. In contrast, phased array head/neck coils and the latest generation parallel imaging array coils are rather straightforward to use in clinical routine. The area covered is large and evaluation of the primary tumor and lymph nodes in the neck is possible within a reasonable time. Therefore, in most institutions, phased array or parallel imaging array coils are used for routine MR imaging scanning of laryngeal and hypopharyngeal cancers. At the authors' institution, we use parallel imaging array coils which combine 64 or 20 channel head coils (for 3T and 1.5T, respectively) with flexible superficial coils placed on the anterior neck.

According to the literature, a slice thickness of 3 to 4 mm is recommended for MR imaging of the larynx/hypopharynx as a compromise between a decreased signal-to-noise ratio due to thinner slices (in particular at 1.5T) and an increased acquisition time necessary to cover the required anatomic area. The recommended in-plane resolution is in the range of 0.4 $\times$ 0.4 mm to 0.8 $\times$ 0.8 mm,[7,11] whereas local circular surface coils placed around the larynx may achieve an in-plane resolution as high as 0.2 $\times$ 0.5 mm.[12,23]

Although MR imaging protocols are subject to rapid technical evolutions, at the authors' institution routine MR imaging protocols for the larynx and hypopharynx include coronal short tau inversion recovery (STIR) followed by axial DWI, T2, and precontrast and postcontrast T1, as well as additional acquisitions in the coronal and/or sagittal plane. DWI is routinely performed with a single shot echoplanar imaging (SS-EPI) sequence with 2 b values (b = 0 and b = 1000) and with apparent diffusion coefficient (ADC) maps generated automatically by the MR imaging software. The imaging protocols from the authors' institution are shown in **Table 1**. Tips and tricks to optimize image quality include the following:

- The comfortably immobilized patient should be instructed to breathe regularly and not too deep and, whenever possible, with an open mouth during image acquisition (as swallowing is not possible with an open mouth)
- The patient should clear the throat between sequences (to avoid coughing during image acquisition)
- Axial images should be strictly parallel to the plane of the true vocal cords (based on sagittal and coronal localizers)

Table 1
Summary of the MR imaging protocol for laryngeal and hypopharyngeal cancer at the authors' institution

Series Number	Sequence Type	Plane	Slice Thickness	Phase Encoding
Series 1	Survey/localizer	Axial, coronal, sagittal		
Series 2	T2 STIR	Coronal	3 mm	Caudal-cranial
Series 3	DWI SS-EPI 2b values (0 and 1000)	Axial	3 mm	Anteroposterior
Series 4	T2 TSE/FSE	Axial	3 mm	Anteroposterior
Series 5	T1 TSE/FSE	Axial	3 mm	Anteroposterior
Series 6[a]	Perfusion T1 cartography (vibe T1 map)	Axial	3 mm	Anteroposterior
Injection: iv. Contrast				
Series 7[a]	Perfusion T1 dynamic vibe	Axial	3 mm	Anteroposterior
Series 8	T1 TSE/FSE	Axial	3 mm	Anteroposterior
Series 9	T1 TSE/FSE with fat saturation	Axial	3 mm	Anteroposterior
Series 10[b]	T1 Dixon	Coronal/sagittal	3 mm	Caudal-cranial

Routinely, a subtraction series (subtracting series 5 from series 8) is obtained by postprocessing to evaluate the enhancement patterns more precisely.
[a] Series 6 and 7 are routinely performed in the post-treatment setting, otherwise optional.
[b] Depending on tumor localization and findings on previous images, either coronal or sagittal or both coronal and sagittal imaging planes are acquired.

- The smallest possible field of view should be chosen (dependent on neck morphotype, 16 × 18 cm – 18 × 20 cm) and an acquisition matrix of 350 to 512 × 450 to 512 should be used
- The phase encoding gradient should be either in the anteroposterior direction (axial and sagittal plane) or in the caudal-cranial direction (coronal plane) to move flow artifacts (especially after iv. contrast) away from the larynx and hypopharynx
- Meticulous shimming for DWI sequences is a must

KEY ANATOMIC CONSIDERATIONS AND IMPLICATIONS FOR PATTERNS OF SUBMUCOSAL TUMOR SPREAD

Accurate radiological assessment of submucosal tumor spread plays a key role in the T classification of laryngeal and hypopharyngeal cancers and in treatment planning, especially for transoral laser excision, open partial laryngectomy, and highly focused radiotherapy. Although knowledge of the anatomy of the larynx and hypopharynx is essential for the correct interpretation of MR imaging scans, a detailed review of the pertinent anatomy is beyond the scope of this article. Nevertheless, to understand what the referring physician needs to know and to deliver actionable information to the patient care team, the clinically relevant anatomy of the paraglottic space, pre-epiglottic space, and laryngeal cartilages will be reviewed.

Paraglottic Space

The paraglottic space plays an important role in the T classification of laryngeal cancers because if it is invaded, SCC is classified as T3 according to the AJCC/UICC guidelines.[8,9] Whether neoplastic involvement of the paraglottic space influences the outcome after radiotherapy is still a matter of debate.[25–27] However, invasion of the posterior paraglottic space and of the thyrocricoarytenoid space (TCAS, see below) is associated with a poorer outcome in terms of overall survival, disease-free survival, and locoregional control after radiotherapy and open partial laryngectomy.[28,29] Furthermore, if the posterior paraglottic space is invaded, transoral laser surgery is contraindicated.[12,23,30]

The paired and symmetric paraglottic space found in the supraglottic and glottic region (**Fig. 1**) mainly contains adipose tissue, loose

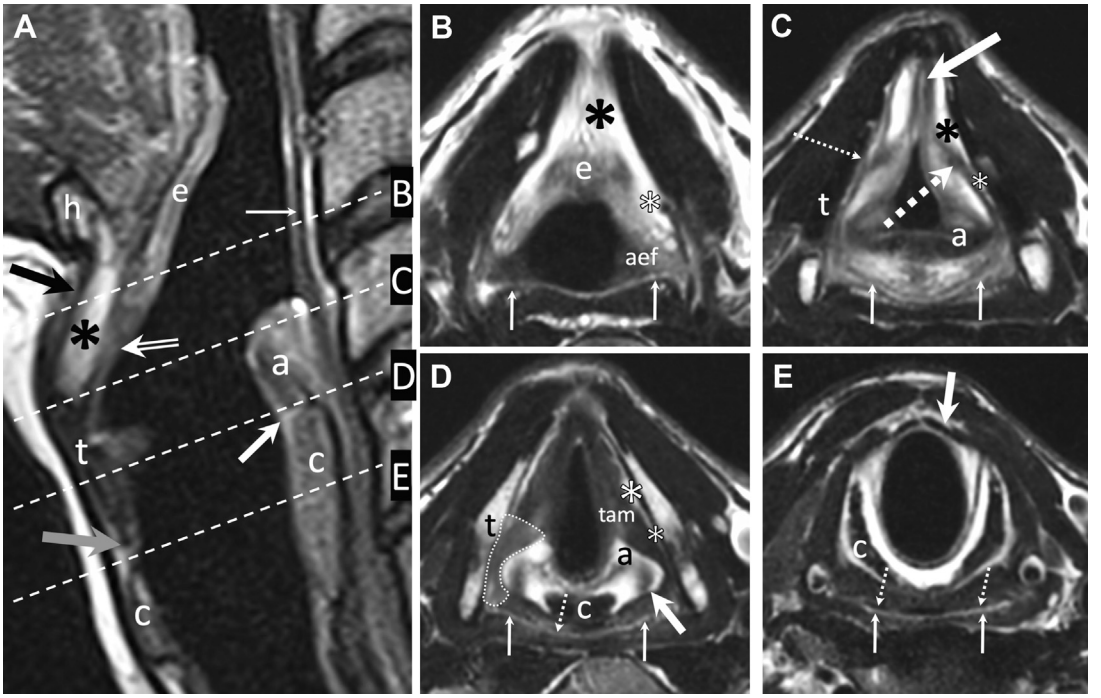

Fig. 1. Normal MR imaging anatomy of the larynx and hypopharynx (T2 images without fat saturation). Paramedian sagittal image (*A*) showing the hyoid bone (h), epiglottis (e), thyroid (t), cricoid (c), and arytenoid (a) cartilages and pre-epiglottic space (*asterisk*). Thick white arrow indicates the cricoarytenoid joint; thin white arrow indicates the posterior hypopharyngeal wall; black arrow indicates the thyrohyoid membrane; double white arrow indicates the thyroepiglottic ligament located inferiorly to the epiglottis; gray arrow indicates the cricothyroid membrane; and dashed white lines indicate the axial planes of images B to E. (*B*) Upper supraglottic region. The pre-epiglottic space (*black asterisk*) is located anteriorly to the epiglottis (e). No clear boundary with the paraglottic space (*white asterisk*) is present at this level. Aryepiglottic fold (aef), posterior hypopharyngeal wall (*thin arrows*). (*C*) Lower supraglottic region (false cord level). The pre-epiglottic space (*black asterisk*) lies laterally to the thyroepiglottic ligament (*thick white arrow*) and anteriorly to the paraglottic space (*white asterisk*). The thyroglottic ligament (*thin dashed arrow*) separates the pre-epiglottic space from the paraglottic space. Thyroarytenoid and aryepiglottic muscle fibers (*thick dashed arrow*) merge with the thyroglottic ligament. Arytenoid cartilage (a). Collapsed lumen of the piriform sinuses (*thin white arrows*). (*D*) True vocal cord level. The thyroarytenoid muscle (tam) makes up the bulk of the true vocal cords. Paraglottic space (*white asterisks*). Arytenoid cartilage (a) and cricoid cartilage (c) forming the cricoarytenoid joint (*thick arrow*). Thyroid cartilage (t). The area surrounded by the thin dashed contours is the TCAS. Dashed arrow points at the retrocricoarytenoid region of the hypopharynx and thin solid arrows point at the posterior hypopharyngeal wall. Note that the posterior parapharyngeal space is bordered posteriorly by the piriform sinuses. (*E*) Subglottic region. Cricoid cartilage (c). Cricothyroid membrane (*thick arrow*). Dashed arrows point at the retrocricoarytenoid region of the hypopharynx and solid thin arrows point at the posterior hypopharyngeal wall.

elastic and collagen tissue, and blood vessels.[31–33] Laterally, the paraglottic space is bordered by the thyrohyoid membrane, thyroid cartilage, and cricothyroid membrane, medially by the quadrangular membrane, laryngeal ventricle, aryepiglottic muscle, and thyroarytenoid muscle (which forms the bulk of the true vocal cords), posteriorly by the mucosa of the piriform sinuses and inferiorly by the conus elasticus. In the posterosuperior supraglottic region, there is no boundary between the paraglottic space and the pre-epiglottic space. However, in the posteroinferior supraglottic region, the thyroglottic ligament (a fibrous septum which fans out from the vocal ligament to the thyroid cartilage) separates the 2 spaces.[31–33] At the glottic level, the paraglottic space can be divided into an anterior part (two-thirds) and a posterior part (one-third) by a line extending laterally from the vocal process of the arytenoid to the thyroid lamina. The posterior paraglottic space is currently considered as part of the TCAS (see **Fig. 1**) and neoplastic invasion of TCAS is an important adverse prognostic factor in laryngeal cancer.[28,29,34]

The paraglottic space is best assessed on axial and coronal images. It is easily identified on MR

imaging because of its high fat content and, therefore, has a high signal intensity on T1 and T2 (see Fig. 1). The normal paraglottic space may show some minor enhancement after iv. administration of gadolinium chelates as it contains blood vessels. MR imaging is superior to CT for assessing the narrow paraglottic space at the vocal cord level.[23,34,35]

The paraglottic space plays a pivotal role in submucosal tumor dissemination and it constitutes a "highway" for submucosal tumor spread. Invasion of the paraglottic space occurs whenever SCC arising in the laryngeal ventricle, false cords, or true vocal cords spreads laterally or whenever SCC of the piriform sinus spreads anteriorly. Key points of submucosal tumor spread along the paraglottic space include the following:

- Tumor spread in the paraglottic space typically occurs in a vertical direction (transglottic spread; Fig. 2).
- Lateral tumor spread from the paraglottic space results in thyroid cartilage invasion.
- Lateral tumor spread from the paraglottic space through the cricothyroid ligament inferiorly and thyrohyoid membrane superiorly leads to invasion of extralaryngeal soft tissues (see Fig. 2).
- Tumor spread from the posterior paraglottic space leads to early involvement of the piriform sinus, cricoarytenoid joint, and posterior thyroarytenoid muscle.

Pre-epiglottic Space

The pre-epiglottic space plays an important role in the T classification of laryngeal cancers: if the pre-epiglottic space is invaded, SCC is classified as T3 according to AJCC/UICC guidelines.[8,9] Multiple authors have suggested that the degree of invasion of the pre-epiglottic space influences surgical options and to a moderate degree the likelihood of local recurrence after radio(chemo)therapy and open partial laryngectomy although others have questioned the impact of pre-epiglottic space invasion on local control after concurrent radiochemotherapy.[36–40]

The pre-epiglottic space mainly contains fatty tissue, some loose connective tissue, and blood vessels (see Fig. 1). Anteriorly, it is bounded by

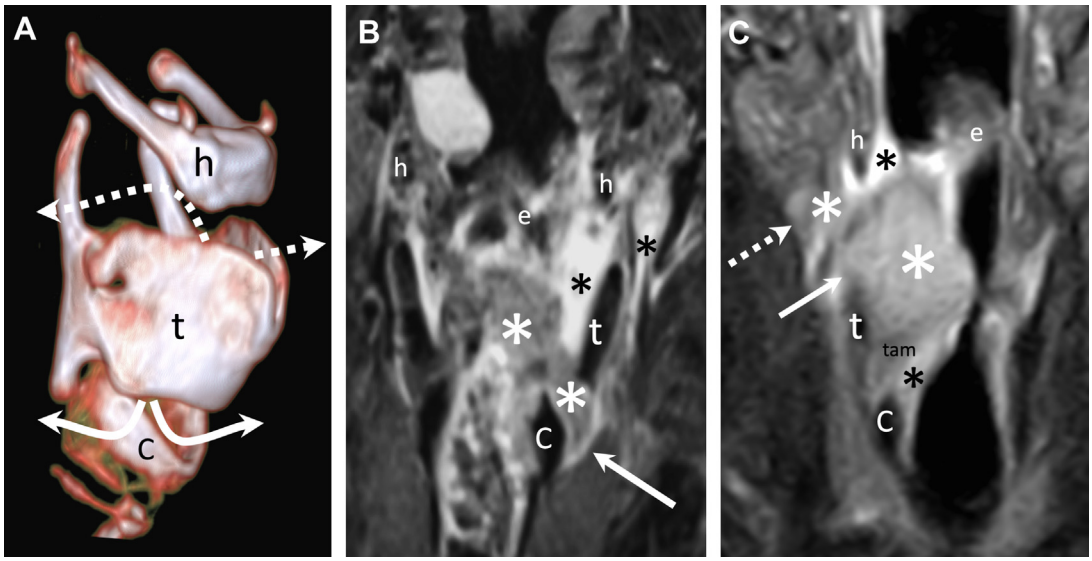

Fig. 2. Key patterns of tumor spread along the paraglottic space and pre-epiglottic space. (*A*) Diagram based on a 3D volume rendering reconstruction of laryngeal cartilages showing extralaryngeal patterns of spread through the cricothyroid membrane (*arrows*) and thyrohyoid membrane (*dashed arrows*). The following annotations apply to all figure parts: hyoid bone (h), thyroid cartilage (t), cricoid cartilage (c), epiglottis (e). (*B*) Coronal T2 STIR image showing a SCC with intermediate signal intensity (*white asterisks*), transglottic spread along the left paraglottic space and extension through the cricothyroid membrane into the extralaryngeal soft tissues (*arrow*). Note areas of very high signal intensity in the left supraglottic larynx and outside the larynx (*black asterisks*) corresponding to peritumoral inflammation. (*C*) Coronal T2 STIR image in another patient with a SCC (*white asterisks*) with moderately high signal intensity invading the pre-epiglottic space, paraglottic space, and right thyroarytenoid muscle (tam). Note lateral tumor spread through the thyrohyoid membrane into the soft tissues of the neck (*dashed arrow*) and destruction of the superior border of the right thyroid cartilage (*arrow*). Very high signal intensity areas (*black asterisks*) surrounding the tumor and corresponding to peritumoral inflammation.

the thyrohyoid membrane and thyroid cartilage, posteriorly by the epiglottis, cranially by the hyoepiglottic ligament, and caudally by the thyroepiglottic ligament.[31–33] It is important to bear in mind that the pre-epiglottic space extends not only anteriorly to but also posterolaterally to the epiglottis and the posterolateral border of the pre-epiglottic space on axial images is located at about the anteroposterior midpoint of the thyroid lamina.[33] The pre-epiglottic space is best seen on axial and sagittal images and it is easily identified on MR imaging and CT because of its high fat content (see **Fig. 1**) The normal pre-epiglottic space behaves like fatty tissue on MR imaging. Minor reticulated contrast enhancement of the pre-epiglottic space can be seen on high-resolution contrast-enhanced T1 because of the presence of blood vessels and loose connective tissue. Early invasion of the pre-epiglottic space occurs when SCC arising from the laryngeal surface of the epiglottis spreads in an anterior direction. Key points of submucosal tumor spread involving the pre-epiglottic space include the following:

- As there is no effective boundary posterosuperiorly between the pre-epiglottic space and paraglottic space, tumor spread from the pre-epiglottic space can result in paraglottic space invasion and vice versa
- Anterolateral tumor spread from the pre-epiglottic space through the thyrohyoid membrane results in invasion of extralaryngeal soft tissues (see **Fig. 2**).

Laryngeal Cartilages

Invasion of the thyroid and cricoid cartilages influences the T classification of laryngeal and hypopharyngeal cancers.[8,9] Laryngeal SCC with invasion of the inner cortex of the thyroid cartilage is classified as T3, whereas laryngeal SCC with invasion of the cricoid cartilage or invasion through the outer cortex of the thyroid cartilage is classified as T4a. In contrast, hypopharyngeal SCC invading the thyroid or cricoid cartilage is classified as T4a irrespective of the degree of cartilage invasion. In addition, invasion of the laryngeal cartilages affects prognosis after radiotherapy and influences the choice of surgery (total laryngectomy vs open partial laryngectomy or transoral laser microsurgery).[4,41]

The thyroid, cricoid and arytenoid cartilages (with the exception of the vocal process of the arytenoids which contains elastic fibrocartilage) are composed of hyaline cartilage (**Fig. 3**). Hyaline cartilage undergoes ossification with increasing age.[42] Ossified cartilage corresponds histologically to bone: it has an inner and outer cortex and a marrow cavity with predominantly fatty tissue, some erythropoietic marrow and bone trabeculae (see **Fig. 3**). Although the normal ossification process of laryngeal cartilages tends to follow a predefined pattern and can result in complete ossification of the thyroid and cricoid cartilage, in most individuals, the central thyroid laminae and parts of the cricoid cartilage remain nonossified throughout life, and differences in ossification between right and left are common.[42,43] Furthermore, asymmetric ossification can be equally seen in normal arytenoid cartilages.[44]

The mechanism by which cancer invades laryngeal cartilages[45–47] involves the following steps:

- An inflammatory phase (with edema and increased vascularization) within the cartilage located in immediate tumor vicinity and before actual tumor invasion
- An osteoblastic phase with new bone formation
- An osteoclastic phase in which newly formed bone is eroded and frank invasion by tumor cells occurs.

Both early neoplastic cartilage invasion and inflammatory changes in the laryngeal cartilages due to tumor vicinity may manifest with increased cartilage ossification (sclerosis) at CT.[6] Therefore, the distinction between the normal mix of nonossified and ossified cartilage, sclerosis due to tumor invasion and sclerosis due to peritumoral inflammation is not possible with CT. Normal nonossified hyaline cartilage and ossified cartilage display characteristic signal intensities on MR imaging (see **Fig. 3**). Hyaline nonossified cartilage and the cortex of ossified cartilage are strongly hypointense on T1 and T2 and do not enhance after iv. contrast administration, whereas the marrow cavity of ossified cartilage behaves like fatty marrow elsewhere in the body. On DWI, normal cartilages have a low signal on b1000 images and on ADC maps (see **Fig. 3**). These characteristic features on MR imaging and the increased capability of MR imaging to distinguish between tumor and peritumoral inflammatory changes (see below) greatly facilitate the assessment of laryngeal cartilage abnormalities and thus avoids diagnostic pitfalls related to CT.

MR IMAGING FINDINGS IN LARYNGEAL AND HYPOPHARYNGEAL CANCER

Tumor and Peritumoral Inflammation

Both primary and recurrent laryngeal and hypopharyngeal SCCs show characteristic signal intensity patterns on MR imaging: an intermediate signal intensity on T1, T2, and STIR and moderate

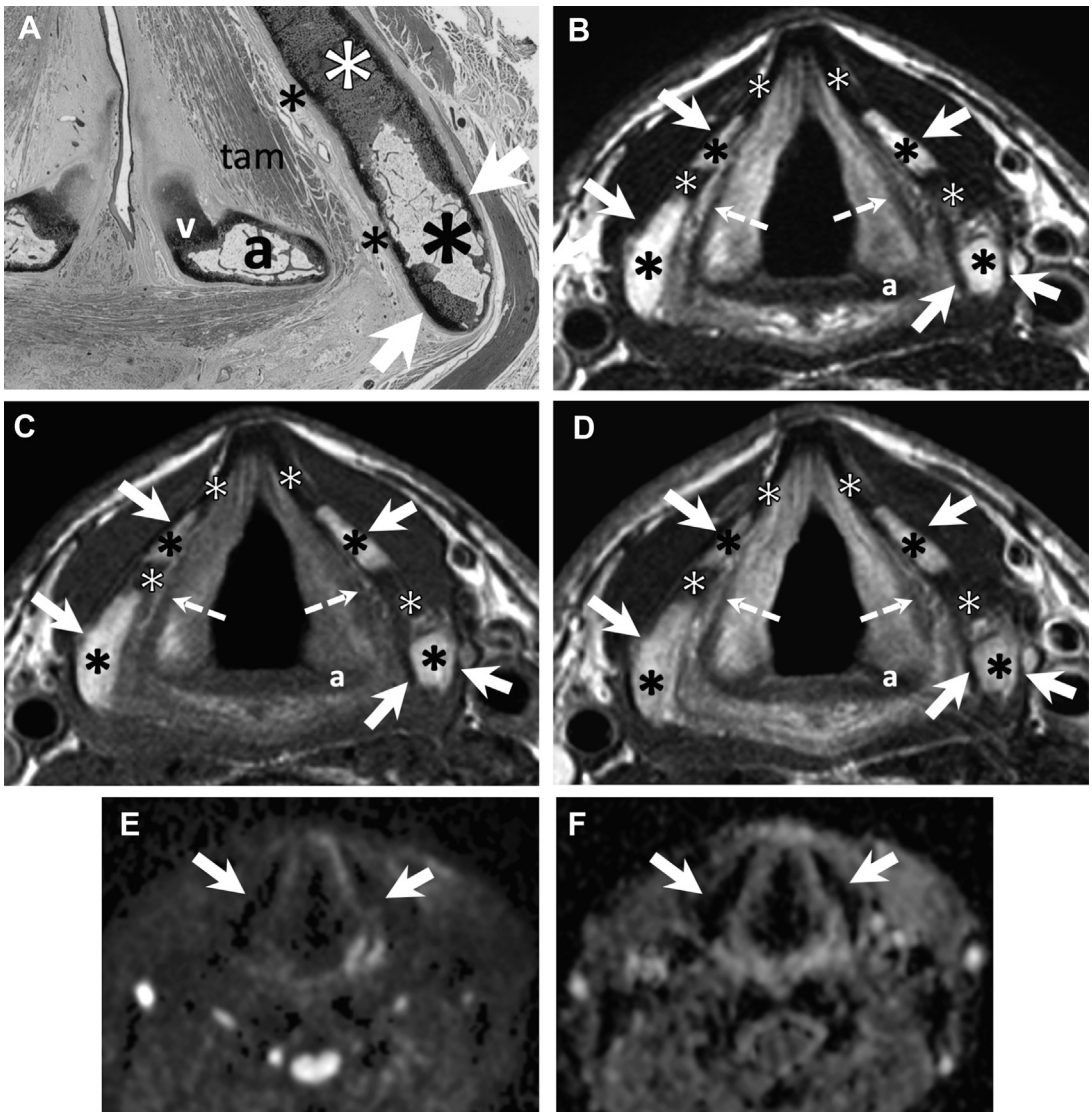

Fig. 3. Normal anatomy of the laryngeal cartilages. (*A*) Whole organ histologic slice at the false cord level. The thyroid cartilage is composed of hyaline nonossified cartilage (*white asterisk*) and of ossified cartilage, which has a cortex (*white arrows*) and a marrow cavity containing adipose tissue and bone trabeculae (*large black asterisk*). Small black asterisks indicate the posterior paraglottic space. Thyroarytenoid muscle fibers (tam) merged with the thyroglottic ligament laterally, body of the arytenoid cartilage (a) and vocal process (v). Axial T2 (*B*), T1 (*C*), contrast-enhanced T1 (*D*), b1000 (*E*), and ADC map (*F*) at the false cord level. Nonossified hyaline cartilage (*white asterisks* in *B*, *C*, and *D*) and cortex of ossified cartilage (*white arrows* in *B*, *C*, and *D*) with a very low signal intensity on all sequences. The marrow of ossified cartilage (*black asterisks* in *B*, *C*, and *D*) has the signal intensity of fat and does not enhance. b1000 image (*E*) and ADC map (*F*) show that cartilages have a low signal intensity (*arrows* in *E* and *F*). Dashed arrows in B, C, and D point at fibers of the thyroarytenoid muscle merging with the thyroglottic ligament.

contrast enhancement after iv. administration of gadolinium chelates[7,11] (**Fig. 4**). Primary laryngeal and hypopharyngeal SCCs can be mass-like, they can extend along the mucosal surfaces or they can be diffusely infiltrating at cross-sectional imaging, whereas recurrent SCCs tend to be located beneath an intact mucosa and they display a diffusely infiltrative invasion pattern with indistinct tumor margins (see **Fig. 4**; **Figs. 5** and **6**).[17,18,48,49] This difference can be explained by histologic characteristics as primary laryngeal and hypopharyngeal SCCs have a rather unicentric growth pattern while recurrent tumors have multicentric tumor foci disseminated over large

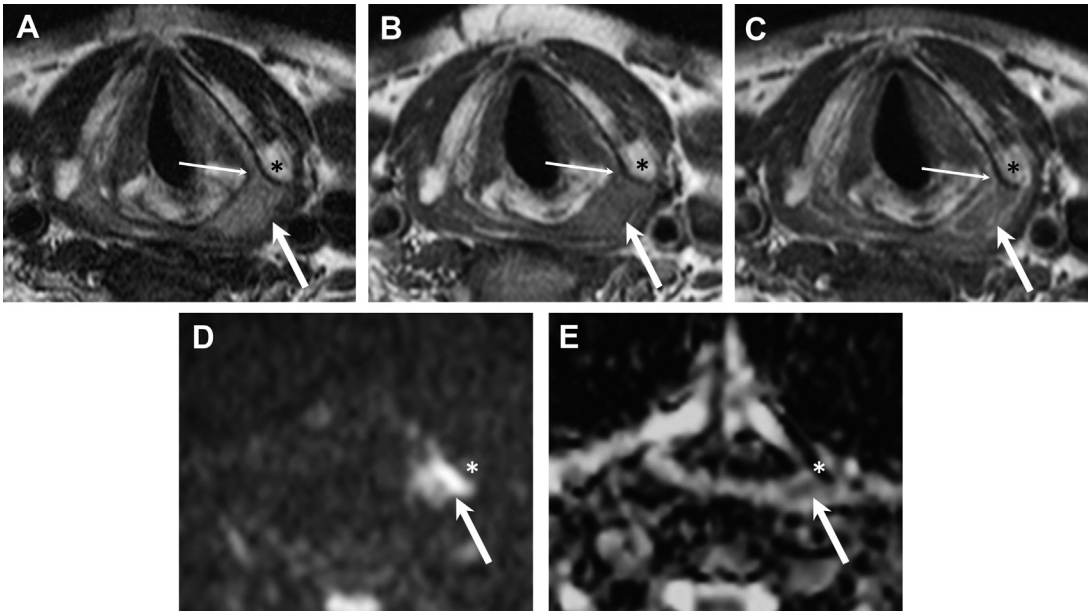

Fig. 4. Small primary SCC arising in the left piriform sinus with characteristic MR imaging features. Axial T2 (*A*), T1 (*B*), contrast-enhanced T1 (*C*), b1000 (*D*) and ADC map (*E*) at the vocal cord level show a mass in the apex of the left piriform sinus (*thick arrows* on all figure parts) with an intermediate signal intensity on T2, low signal intensity on T1 and moderate contrast enhancement. High signal on the b1000 image (*D*) and low signal on the ADC map (*E*) indicate restricted diffusion. Mean ADC was 1.03×10^{-3} mm^2/s. The tumor shows most likely minimal invasion of the posterior paraglottic space (*thin arrow* in *A*, *B*, and *C*). Note a very thin hyperintense rim surrounding the tumor in C corresponding to peri-tumoral inflammation with increased vascularization. Asterisk on all figure parts shows a normal adjacent thyroid cartilage consisting of ossified cartilage.

anatomic areas beneath an intact mucosa.[18,48,49] Restricted diffusion is characteristic for both primary and recurrent SCCs and mean ADC values (calculated with b = 0 and b = 1000) are in the range of 0.9 to 1.3 $\times$ 10^{-3} mm^2/s[19,50,51] (see **Figs. 4** and **6**). Correlation with histopathology has shown that mean ADC values in laryngeal and hypopharyngeal SCCs are significantly correlated with cellularity, stromal component, and nuclear-cytoplasmic ratio, and differences in ADC values between tumors can be mainly explained by variable amounts of tumor stroma components.[52]

Both primary and recurrent SCCs are often surrounded by variable degrees of peritumoral inflammation, which can accompany early and advanced cancers and may lead to overestimation of tumor size unless careful analysis of multiparametric MR imaging signal intensity is done (see **Fig. 2**; **Figs. 7** and **8**). These peritumoral inflammatory changes which precede tumor invasion of adjacent structures are characterized by a higher signal intensity on T2 and STIR and by a stronger contrast enhancement than the tumor itself. Also, on DWI peritumoral inflammation shows no restricted diffusion, and mean ADC values (calculated with b = 0 and b = 1000) are typically in the range of 1.4 to 1.9 $\times$ 10^{-3} mm^2/s.

Using a multiparametric approach with the aforementioned diagnostic criteria, MR imaging with current state-of-the-art coils allows an improved distinction between tumor and peritumoral inflammatory changes, therefore facilitating a more precise evaluation of critical anatomic subsites. Although newer studies found a low CT sensitivity for the detection of neoplastic invasion of the paraglottic space,[35] older studies reported a high sensitivity of MR imaging and CT for the detection of neoplastic invasion of the pre-epiglottic space and paraglottic space.[53–55] However, as older studies have used different morphologic criteria that do not allow distinction between tumor and inflammation, the reported specificity of MR imaging and CT in the paraglottic space was low (around 50%), thus leading to overestimation of tumor spread in a considerable number of cases.[54–56] Nevertheless, using the aforementioned MR imaging criteria, which take differences in signal intensity, contrast enhancement, and DWI characteristics into consideration, it is currently possible to distinguish between tumor and inflammation in the paraglottic space and in the TCAS with a sensitivity of 100% and a specificity of 78%.[34] This area, which has important prognostic implications, is particularly difficult to evaluate on CT scans.[35] Although other

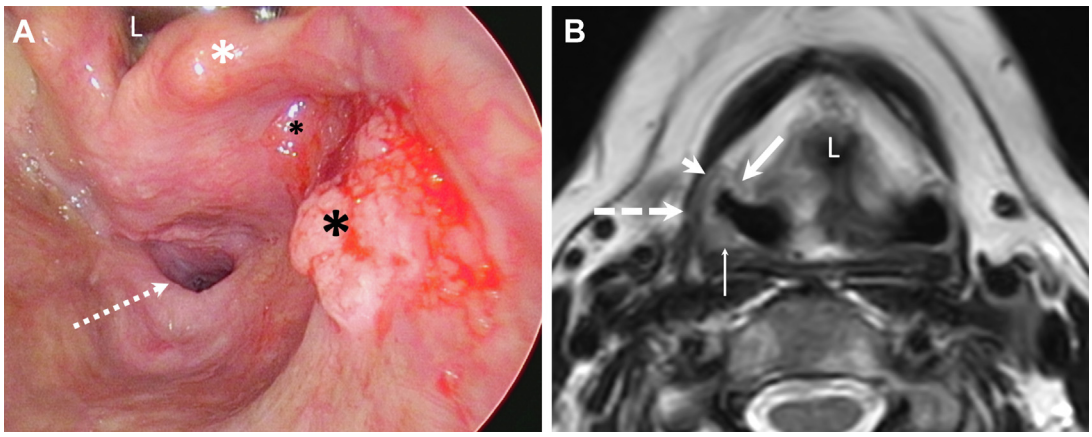

Fig. 5. Primary SCC arising in the right piriform sinus with a characteristic superficial pattern of spread. Endoscopic view (*A*) showing a right piriform sinus tumor involving the anterior wall of the piriform sinus (*small black asterisk*), the angle, the lateral wall (*large asterisks*), and with beginning spread on the posterior wall. Aryepiglottic fold (*large white asterisk*). Laryngeal lumen (L). Dashed arrow points at the esophageal verge. Note that as we are looking from above, the right piriform sinus appears on the right side of the image. Axial T2 image (*B*) shows the tumor with an intermediate signal intensity spreading along the anterior wall of the piriform sinus, that is, the posterior wall of the aryepiglottic fold (*thick arrow*), the angle (*short arrow*), the lateral wall (*dashed arrow*), and the posterior hypopharyngeal wall (*thin arrow*). Larynx (L). There is minimal invasion of the aryepiglottic fold fat (which is in continuity with the paraglottic space).

areas of the larynx, which contain higher amounts of fat, such as the pre-epiglottic space, are more easily evaluated with CT, it is worthwhile mentioning that currently there are no series in the literature systematically comparing the diagnostic performance of multiparametric DWI MR imaging with CT in the deep laryngeal spaces. Furthermore, because of the difficulty to obtain radiologic-pathologic correlation, most data in the literature are based on older studies, which have used older diagnostic criteria, and newer studies using the aforementioned criteria are based only on a limited number of cases.

Regarding the detection and staging of early SCC of the larynx and hypopharynx, data in the literature are scarce and do not allow to draw solid conclusions about the added value of MR imaging in T1 and T2 lesions.[57] Nevertheless, some authors have pointed out that MR imaging is clearly superior to CT in the preoperative staging of early glottic cancer.[58] It has even been suggested that DWI may detect changes in tumor size and shape before they become apparent at laryngostroboscopy and may help to distinguish laryngeal SCC from precursor lesions.[59]

Neoplastic Cartilage Invasion

Detection of neoplastic cartilage invasion at CT uses the criteria of sclerosis, erosion/lysis, and extralaryngeal spread.[6] Sclerosis is a sensitive but nonspecific sign of cartilage invasion, especially in the thyroid cartilage (specificity = 40%).[6] In contrast, erosion/lysis and extralaryngeal spread are specific signs (specificity = 93%) but not sensitive as they are bound to the presence of more advanced invasion of laryngeal cartilages. In the presence of sclerosis alone, it is nearly impossible to decide, whether sclerosis corresponds to cartilage invasion, whether it is caused by peritumoral inflammation with bone remodeling, or whether it corresponds to asymmetric ossification. Furthermore, it has been shown that the positive predictive value of CT to detect major cartilage invasion and extralaryngeal spread is limited and varies between 53% and 81%[6,60,61] (**Fig. 9**). Another problem with CT is that nonossified cartilage can have similar attenuation values as SCC on contrast-enhanced CT rendering a correct radiologic interpretation difficult (**Fig. 10**). Applying the diagnostic criteria for tumor, inflammation, normal non-ossified, and normal ossified cartilage as explained earlier, MR imaging allows an improved diagnosis of cartilage abnormalities thus avoiding diagnostic pitfalls related to CT (see **Fig. 10**; **Figs. 11** and **12**). In summary, if a cartilage in the immediate tumor vicinity displays a moderately high signal intensity on T2, a moderate enhancement on contrast-enhanced T1 and restricted diffusivity, the cartilage should be regarded as invaded (see **Fig. 12**). However, if a cartilage in the immediate tumor vicinity displays a higher signal intensity on T2 and a stronger enhancement than the adjacent

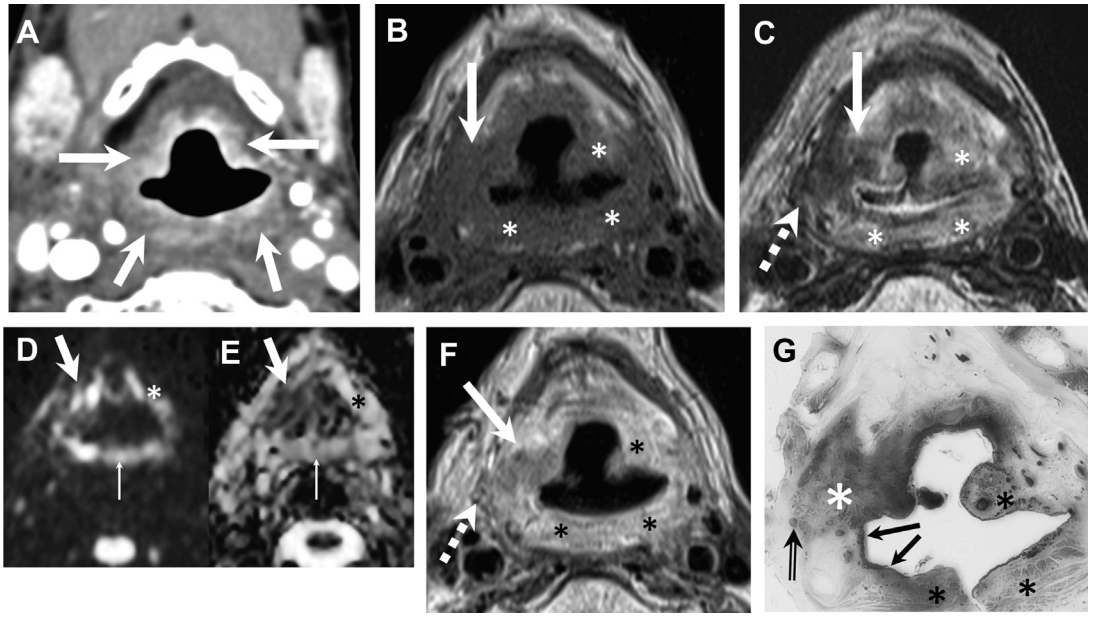

Fig. 6. Characteristic MR imaging findings in a recurrent supraglottic SCC after radiation therapy. The recurrent tumor was missed at initial endoscopy and CT but was correctly diagnosed at MR imaging. Axial contrast-enhanced CT at the supraglottic level (*A*) shows nonspecific, diffuse, and symmetric contrast enhancement surrounding the supraglottic larynx and the posterior hypopharyngeal wall (*arrows*). Findings were similar to those of a previous CT obtained 6 months earlier (not shown). Corresponding axial T1 (*B*), T2 (*C*), b1000 (*D*), ADC (*E*), and contrast-enhanced T1 (*F*) images obtained at the same level show a poorly defined, infiltrative lesion (*white arrows* in *B*, *C*, *D*, *E*, and *F*) involving the right aryepiglottic fold with invasion of the right pre-epiglottic and paraglottic space. The lesion has a low signal intensity on T1, intermediate signal intensity on T2, moderate enhancement and restricted diffusion strongly suggesting recurrent tumor. ADC was 1.12×10^{-3} mm^2/s. There is extralaryngeal spread through the thyrohyoid membrane (*dashed arrows* in *C* and *F*). The retropharyngeal space (*asterisks* in *B*, *C*, *F* and *thin arrows* in *D* and *E*) and the left aryepiglottic fold (*asterisks* on *B*, *C*, *D*; *E* and *F*) show edema with low signal intensity on T1, slightly higher signal intensity than the tumor on T2, no restricted diffusion, and stronger enhancement than the tumor on contrast-enhanced T1. Note also intermediate signal on T2 along the antero-posterior wall of the piriform sinus. This finding was considered suspicious of tumor involvement but could not be confirmed on the other MR imaging sequences. Corresponding whole organ histologic slice (*G*) confirms recurrent SCC. Tumor (*white asterisk*) invading the right pre-epiglottic and paraglottic space. Inflammatory edema (*black asterisks*). Neoplastic involvement of extralaryngeal soft tissues (*double arrow*) on the right. There was also superficial tumor spread along the mucosa of the right piriform sinus (*solid arrows*) as suspected on T2.

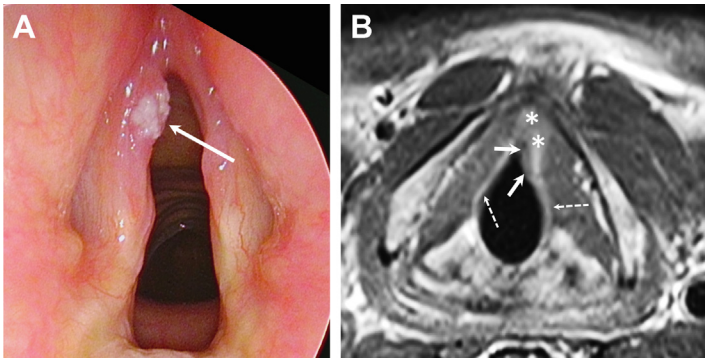

Fig. 7. T1a glottic SCC with peritumoral inflammatory changes. Endoscopic view (*A*) showing a small SCC (*arrow*) located in the anterior third of the left vocal cord. Vocal cord mobility was normal. Note that as we are looking from above, the left vocal cord appears on the left side of the image. Axial contrast-enhanced T1 image (*B*) shows the small and superficial tumor of the anterior left vocal cord with moderate enhancement (*solid arrows*). The tumor is surrounded by an area of stronger enhancement than the tumor itself (*asterisks*) corresponding to peritumoral inflammation. Note that tumor enhancement is also lower than the enhancement of the mucosa overlying the rest of the vocal cords (*dashed arrows*). The thyroarytenoid muscle and the paraglottic space are not invaded by the tumor.

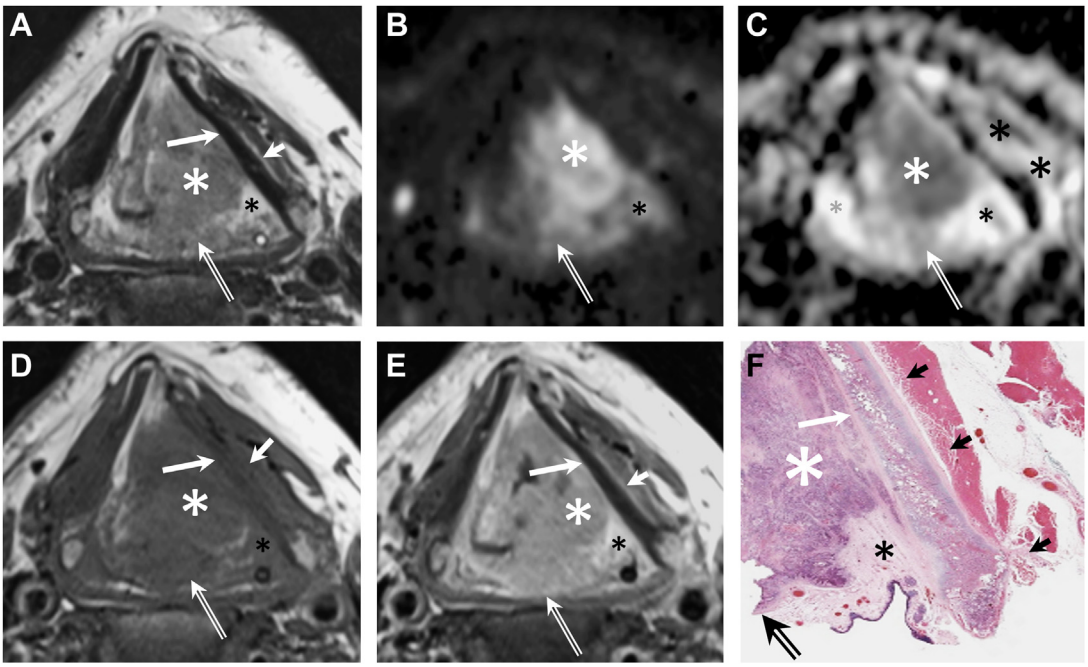

Fig. 8. Left supraglottic SCC with peritumoral inflammation and invasion of the paraglottic space. Axial T2 (*A*), b1000 (*B*), ADC (*C*), T1 (*D*), and contrast-enhanced T1 (*E*) obtained at the supraglottic level show a tumor arising from the left false cord with intermediate signal on T2, restricted diffusion, and moderate contrast enhancement (*white asterisk* on all figure parts). Tumor invasion of the retrocricoarytenoid region (*double arrow* on all figure parts) and of the anterior two-thirds of the left paraglottic space (*long solid arrow* on on *A*, *D* and *E*). The posterior left paraglottic space shows inflammation (*black asterisk* on all figure parts). The adjacent thyroid cartilage shows a low signal intensity on all sequences, which corresponds to normal nonossified hyaline cartilage. Note a thin rim of inflammation extending along the outer lamina of the left thyroid cartilage (*short arrows* on *A*, *D*, *E* and *large black asterisks* on *C*). Edema of the right posterior paraglottic space (*gray asterisk* on *C*). Detail from whole organ histologic slice (*F*) confirms all MR imaging findings. SCC (*white asterisk*) invading the anterior paraglottic space (*long white arrow*) and the retrocricoarytenoid region (*double arrow*). There was no invasion of the nonossified thyroid cartilage histologically. Inflammation in the right posterior paraglottic space (*black asterisk*) and of the strap muscles along the outer thyroid lamina (*short arrows*).

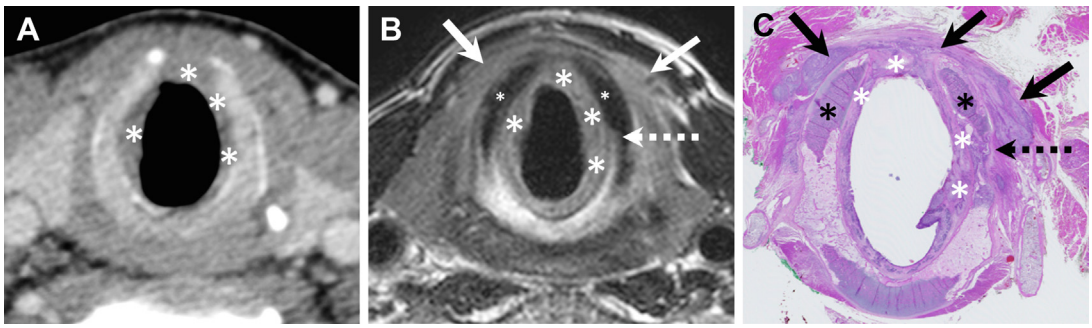

Fig. 9. Extralaryngeal spread missed on CT and detected by MR imaging in a glottic SCC. Axial contrast-enhanced CT (*A*) at the subglottic level shows nearly circumferential subglottic tumor spread (*asterisks*). The cricoid cartilage is poorly ossified and does not show signs of cartilage invasion. The extralaryngeal soft tissues were interpreted as normal. Corresponding T2 image (*B*) shows subglottic tumor spread (*large asterisks*). The anterior portion of the cricoid cartilage is composed of nonossified cartilage (*small asterisks*). Note an irregular contour on the left suspicious of cartilage invasion (*dashed arrow*). In addition, there is massive bilateral extralaryngeal tumor spread (*arrows*) not revealed by CT. Corresponding whole organ histologic slice (*C*) confirms MR imaging findings. Subglottic tumor (*white asterisks*). Nonossified cricoid cartilage (*black asterisks*). Invasion of nonossified hyaline cartilage (*dashed arrow*). Bilateral anterior extralaryngeal tumor spread (*arrows*) mainly occurring through the cricothyroid membrane.

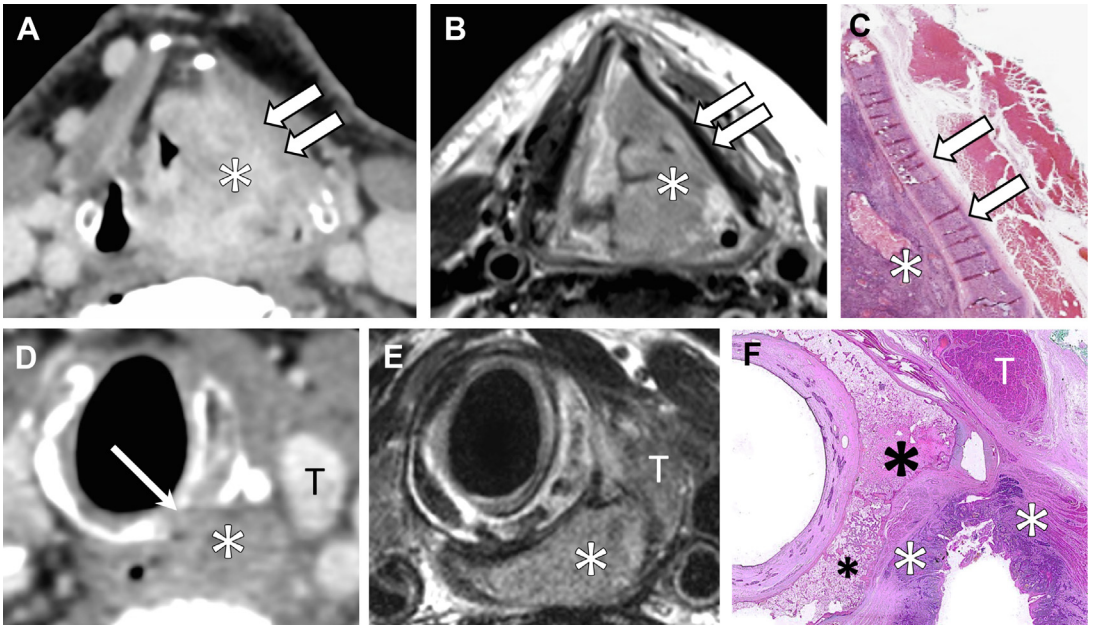

Fig. 10. Pitfalls related to similar attenuation values of SCC and nonossified hyaline cartilage on CT and avoided by MR imaging. Upper figure row (*A–C*) shows images of a patient with supraglottic SCC. Axial contrast-enhanced CT shows a tumor (*white asterisk*) invading the left paraglottic space and abutting the left thyroid lamina (*white arrows*). The thyroid lamina has similar attenuation values as the tumor. Cartilage invasion cannot be ruled out. Corresponding contrast-enhanced T1 image (*B*) shows that the tumor (*asterisk*), which invades the paraglottic space has an intermediate signal intensity, whereas the left thyroid lamina is strongly hypointense suggesting normal nonossified hyaline cartilage. (*C*) Detail from the corresponding histologic slice confirms MR imaging findings. There was tumor invasion of the paraglottic space but no invasion of the nonossified thyroid cartilage. Tumor (*asterisk*). Noninvaded hyaline cartilage (*white arrows*). Lower figure row (*D–F*) shows images of a patient with a piriform sinus tumor invading the esophageal verge. Axial, contrast-enhanced CT image (*D*) shows that the tumor (*asterisk*) is in close vicinity of the cricoid cartilage. The cricoid cartilage has an irregular ossification pattern and an area of osteolysis (*arrow*) is suspected. Thyroid gland (T). Corresponding T2 image obtained at the same level (*E*) shows the tumor with intermediate signal intensity (*asterisk*) surrounded by a hypointense rim. The posterior lamina of the cricoid cartilage shows a mix of ossified and nonossified portions and its cortex is preserved. Thyroid gland (T). Whole organ histologic slice (*F*) reveals absent invasion of the cricoid cartilage. The cricoid cartilage has an irregular ossification pattern with a mix of ossified (*small black asterisk*) and nonossified (*large black asterisk*) portions. Tumor invading the esophageal verge (*white asterisks*). Thyroid gland (T).

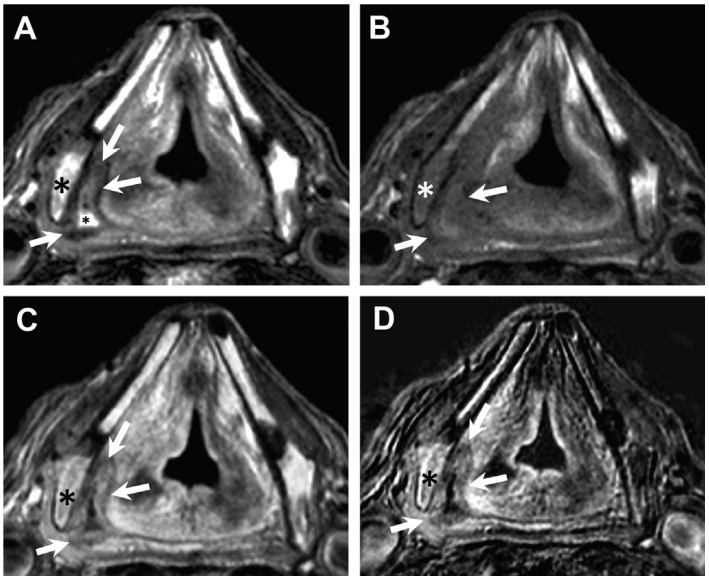

Fig. 11. Characteristic MR imaging features of cartilage inflammation. Patient with an SCC of the right piriform sinus. Axial T2 (*A*), T1 (*B*), contrast-enhanced T1 (*C*), and subtraction image obtained by subtracting T1 from contrast-enhanced T1 (*D*) show a piriform sinus tumor invading the anterior wall, the angle, the lateral wall, and the posterior wall of the piriform sinus (*arrows* on all figure parts). The tumor has an intermediate signal on T2, a low signal on T1, and a moderate enhancement on contrast-enhanced T1. Note that the thyroid cartilage in the immediate tumor vicinity (*asterisk* on all figure parts) shows a much higher signal intensity on T2 than the tumor, a similar low signal on T1, and a much stronger enhancement on T1. The difference in enhancement patterns is particularly well seen in D (subtraction image). Small asterisk in A indicates fluid retention in the right piriform sinus.

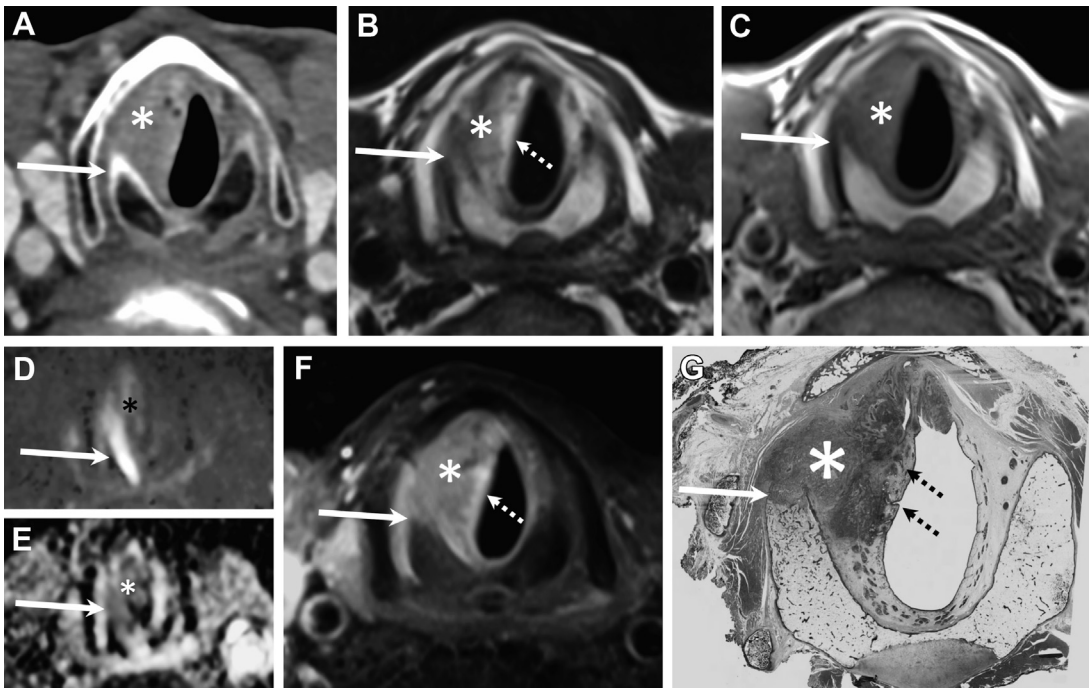

Fig. 12. MR imaging as a problem-solving tool for cartilage sclerosis on CT. Patient with a glottic SCC. Contrast-enhanced CT image (*A*) reveals subglottic tumor spread (*asterisk*) and sclerosis of the adjacent cricoid cartilage (*arrow*). Based on CT findings, it is difficult to decide whether sclerosis corresponds to neoplastic invasion or inflammation. Corresponding axial T2 (*B*), T1 (*C*), b1000 (*D*), ADC (*E*), and contrast-enhanced fat-saturated T1 (*F*) images show that the subglottic tumor has an intermediate signal intensity on T2, low signal intensity on T1, and moderately strong enhancement after iv. contrast (*asterisk* in *B*, *C*, and *F*). Note that the subglottic mucosa overlying the tumor has a stronger signal on T2 and a stronger enhancement than the tumor (*dashed arrows* in *B* and *F*). The adjacent cricoid cartilage, however, has similar signal intensities and similar contrast enhancement as the tumor (*arrows* in *B*, *C*, and *F*), suggesting neoplastic invasion. DWI shows restricted diffusion in the tumor (*asterisk* in D and E) and in the cricoid cartilage (*arrows* in *D* and *E*). Histologic slice (*G*) confirms subglottic submucosal tumor spread (*asterisk*) and neoplastic invasion of the cricoid cartilage (*arrow*). Inflammatory edema beneath the intact lateral subglottic mucosa (*dashed arrows*).

tumor, and if there is no restricted diffusion, the diagnosis of peritumoral cartilage inflammation should be made (see **Fig. 11**). It is worthwhile mentioning that DWI images are not always contributive to the diagnosis due to geometric distortion and lower spatial resolution. Therefore, if DWI images are of insufficient diagnostic quality, in the authors' experience, one should rely on standard morphologic MR imaging images.

DIFFERENTIATING TUMOR RECURRENCE FROM POST-TREATMENT CHANGES

Recurrence in laryngeal SCC is relatively common and depends on age, subsite, stage, histologic differentiation, and treatment modality. Although the recurrence rate is about 5% to 13% in T1 cancer, T3-T4 cancers have a recurrence rate of about 30% to 40%.[62,63] Recurrence most often occurs at the site of the primary tumor and about 90% of recurrences occur within 3 years after primary treatment. In hypopharyngeal SCC, recurrence rates are even higher than in laryngeal SCC and they equally depend on subsite, stage, histologic differentiation, and primary treatment modality.[64] Early detection of recurrent disease plays a major role in a successful disease outcome. Endoscopic and clinical follow-up may overlook recurrent disease, especially after radiotherapy because of radiation-induced edema, fibrosis, or radiation-induced complications, for example, soft tissue necrosis or cartilage necrosis. Biopsy itself can substantially aggravate the situation by precipitating complications due to poor wound healing after biopsy.[17,65] Furthermore, as recurrences after radiotherapy tend to occur under an intact mucosa, endoscopic biopsy may also miss recurrent disease because of the necessity to obtain deep biopsies without being able to identify endoscopically the most appropriate site for tissue sampling.[7]

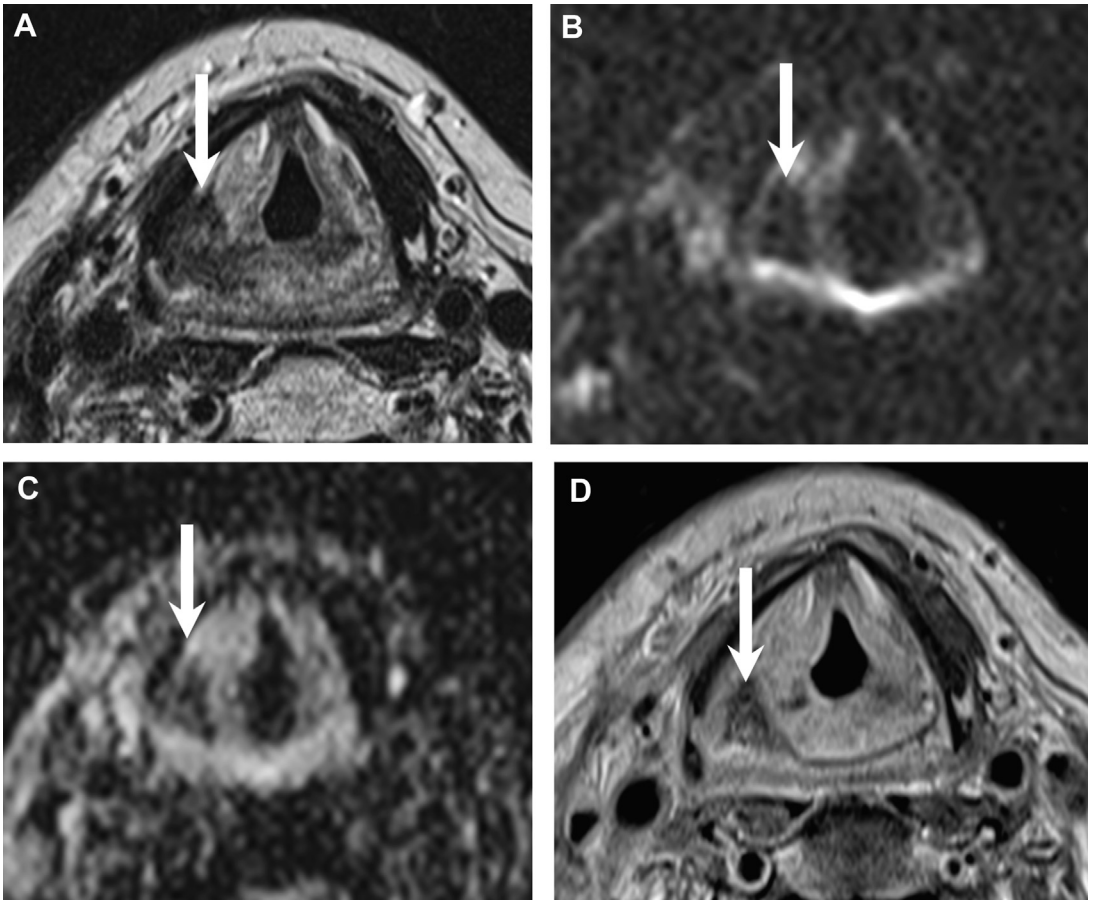

Fig. 13. Characteristic MR imaging features of late fibrosis/post-treatment scar tissue. MR imaging obtained 3 months after radiotherapy for an SCC of the piriform sinus. Axial T2 (*A*), b1000 (*B*), ADC (*C*), and contrast-enhanced T1 (*D*) show a well-defined strongly hypointense area on T2 (similar signal as muscle tissue) with minor contrast enhancement (*arrows* in *A* and *D*). Note low signal on b1000 and ADC map (*arrows* in *B* and *C*) because the tissue is very rich in collagen fibers (T2 blackout effect).

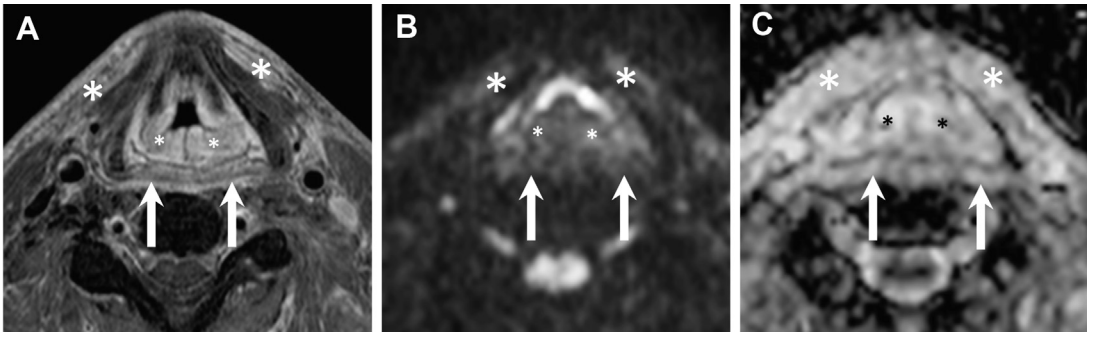

Fig. 14. Characteristic MR imaging features of inflammatory edema after radiotherapy. MR imaging obtained 3 months after radiotherapy for an SCC of the supraglottic larynx. Axial contrast-enhanced fat-saturated T1 (*A*), b1000 (*B*), and ADC (*C*) images show bilateral and symmetric swelling of the aryepiglottic folds with strong contrast enhancement and without restricted diffusion (*small asterisks* on all figure parts) suggesting inflammatory edema. Note also inflammatory edema in the prelaryngeal strap muscles (*large asterisks* on all figure parts), as well as in the hypopharynx and retropharyngeal space (*arrows*).

Several authors have demonstrated the added value of DWI for the detection of residual/recurrent head and neck cancer after radiotherapy in comparison to CT and for distinguishing residual/recurrent disease from benign post-treatment changes; however, they have pointed out that false-positive evaluations caused by late fibrosis/scar tissue still occurred.[15,66] Other authors found that major overlap of ADC values measured in benign post-treatment changes and in recurrent laryngeal cancer limited the ability of quantitative DWI to distinguish between the 2 entities.[67] Nevertheless, by carefully combining morphologic MR imaging criteria with DWI, a high diagnostic performance for distinguishing post-treatment residual/recurrent disease from benign changes after radiotherapy (in particular late fibrosis) can be achieved, the positive predictive value and the negative predictive value of DWI MR imaging being as high as 92% and 95%, respectively.[19] Both late fibrosis/mature scar and residual/recurrent disease have low ADC values (around 1×10^{-3} mm^2/s).[19] This diagnostic DWI pitfall can be avoided as their morphologic characteristics are different: recurrent SCC has a moderately high signal intensity on T2 (see **Fig. 6**); however, late fibrosis/mature scar typically displays a very low signal intensity on T2 (lower than or similar to the signal intensity of muscles) and often no or only minor contrast enhancement (**Fig. 13**).[12,19] Furthermore, mature scars/fibrosis tend to have a characteristic linear or triangular shape. Low ADC values in late fibrosis can be explained by the fact that mature scar tissue is mainly composed of densely packed collagen (T2 blackout effect). In contrast, radiation-induced edema typically manifests with symmetric soft tissue swelling of the larynx and hypopharynx, variable contrast enhancement, and no restricted diffusion (**Fig. 14**). Chondronecrosis after radiotherapy has a characteristic aspect on CT with air inclusions and fragmentation of sclerotic cartilages. However, in the presence of associated recurrent disease (in up to 30% of cases), distinguishing between chondronecrosis alone and chondronecrosis with tumor is less straightforward on CT. This diagnostic pitfall can be avoided by combining morphologic MR imaging sequences with DWI.[17] Nevertheless, necrotic debris, pus, and fungal infection in areas of chondronecrosis may also cause restricted diffusion and can be confounded with recurrent disease.

DIFFERENTIAL DIAGNOSIS

Less than 5% of laryngeal and hypopharyngeal tumors are of nonsquamous cell origin. Unlike primary SCC, they are often located beneath an

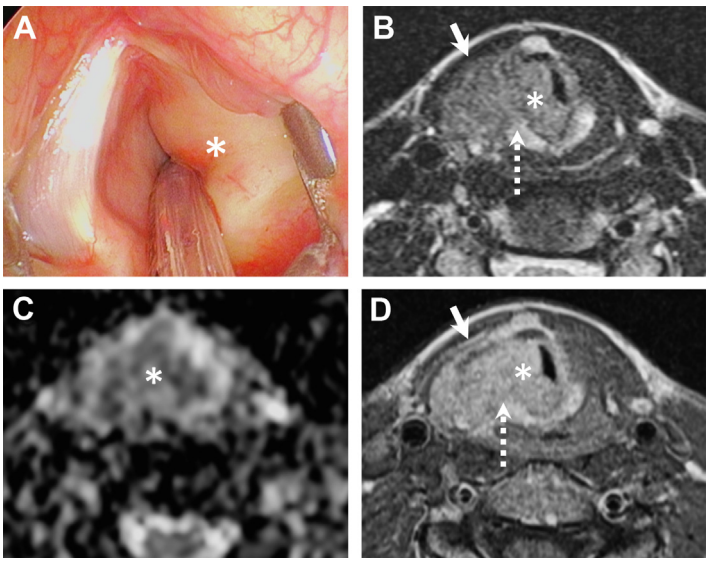

Fig. 15. Rosai-Dorman disease manifesting as a submucosal laryngeal tumor. The patient presented with increasing dyspnea and slight changes in voice quality over 3 months. Endoscopic view (*A*) showing an entirely submucosal lesion involving the right hemilarynx and leading to major subglottic obstruction (*asterisk*). Axial T2 (*B*), ADC (*C*), and contrast-enhanced T1 (*D*) obtained at the subglottic level show an infiltrative lesion involving the right subglottic region (*asterisk*) with an intermediate signal intensity on T2 and restricted diffusion (ADC = 0.7×10^{-3} mm^2/s). Homogeneous and relatively strong enhancement is seen in D. The lesion invades the thyroid cartilage and there is extralaryngeal tumor spread (*arrows* in *B* and *D*). Invasion of the right cricoid (*dashed arrows* in *B* and *D*). An enlarged level IV lymph node was equally seen (not shown). MR imaging suggested the probable diagnosis of lymphoma based on the low ADC, homogeneous enhancement, and the fact that the tumor was entirely submucosal. Biopsy revealed, however, Rosai Dorfman disease.

intact mucosa and sampling errors may occur with endoscopic biopsy.[7,68] The role of imaging mainly consists in confirming a submucosal tumor, determining the precise tumor extent, and guiding the endoscopist to the most appropriate biopsy site to avoid false-negative biopsies. Although some tumors, such as chondrosarcoma, lipoma, schwannoma, melanoma, paraganglioma or vascular lesions (hemangioma and vascular malformations) show characteristic imaging features at MR imaging allowing distinction from SCC,[7,68] other tumor types show overlapping features with SCC and only deep targeted biopsy can differentiate between SCC and non-SCC. Such tumors include adenoid cystic carcinoma, adenocarcinoma, rhabdomyosarcoma, and many more. When lymphoma first presents as a submucosal laryngeal lesion without associated adenopathy (rare presentation), the diagnosis can be quite challenging. However, although the very low ADC values (in the range of 0.5–0.8 $\times$ 10^{-3} mm^2/s) may suggest the diagnosis of lymphoma, biopsy is always required as other rare conditions, such as Rosai Dorfman disease or IgG4 related disease may present with similar MR imaging features (**Fig. 15**). Nevertheless, as a general rule, in patients with a suspected lesion beneath a completely intact mucosa at endoscopy and a tumor mass with similar imaging characteristics as SCC, the radiologist should suggest the diagnosis of an unusual histology.[7,68] It is also worthwhile mentioning that some non-neoplastic conditions, such as tuberculosis, may mimic SCC clinically and at morphologic MR imaging. The diagnosis can be quite challenging in nonendemic areas and in the absence of a known history of tuberculosis or predisposing factors. However, absent restriction of diffusion and pulmonary involvement (**Fig. 16**) in these cases are very helpful in suggesting the diagnosis and contributing to an adequate patient work-up.

WHAT THE REFERRING PHYSICIAN NEEDS TO KNOW

The major goal of radiology reports is to provide accurate, timely, and pertinent information. In many institutions, structured reporting is increasingly used for improved comprehensiveness, to avoid diagnostic errors by omitting key information, for a more consistent evaluation at multidisciplinary

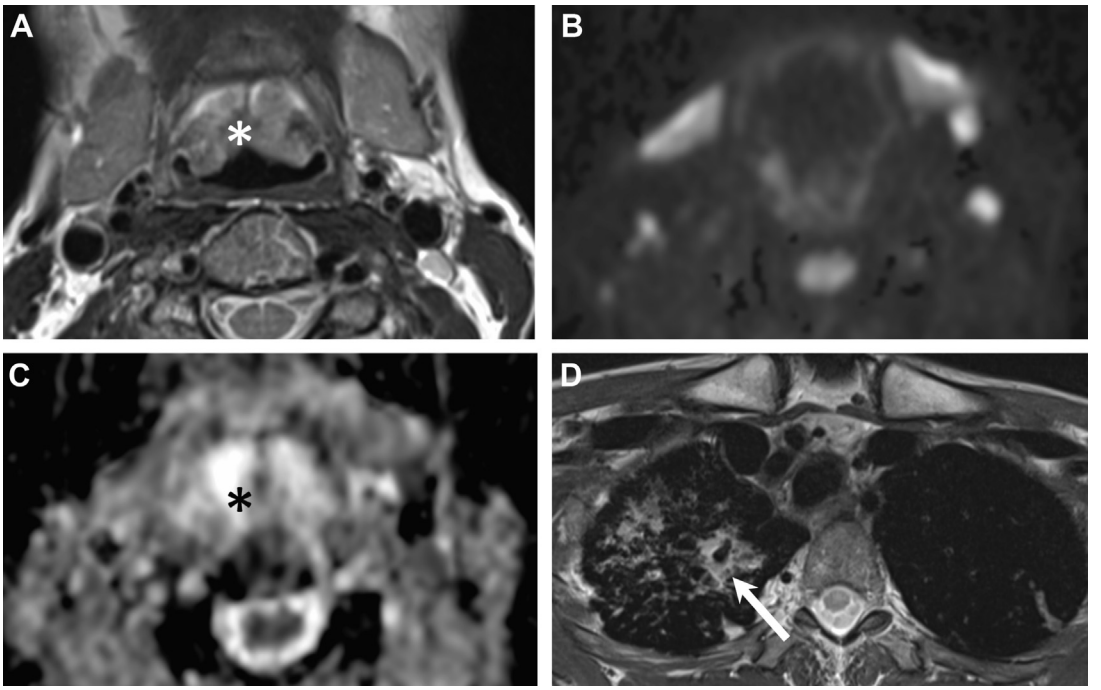

Fig. 16. Tuberculosis of the supraglottic larynx with pulmonary involvement. Patient presenting with hoarseness increasing over several months and some weight loss. Fiberoptic endoscopy showed a bulky and ulcerated lesion of the epiglottis. Before biopsy, an MR imaging was obtained. Axial T2 (*A*) shows an epiglottic lesion infiltrating the pre-epiglottic space (*asterisk*). Corresponding b1000 image (*B*) and ADC map (*C*) show no restriction of diffusivity (*asterisk* in *C*) suggesting an inflammatory lesion. ADC was 1.6 $\times$ 10^{-3} mm^2/s. Axial T2 image (from the same series as image *A*) at the level of the upper mediastinum (*C*) reveals characteristic right pulmonary involvement with cavern formation (*arrow*). The diagnosis of possible tuberculosis was suggested based on MR imaging findings. The diagnosis was confirmed.

tumor boards, for follow-up purposes, and for data collection and research. Structured reporting includes a structured format, consistent organization, and consistent terminology. Even if an IT-based structured reporting template is not available at a radiologist's institution, the following key information using standard terminology as described earlier should be included in every MR imaging report dealing with laryngeal and hypopharyngeal cancer:

- Which anatomic subsites of the larynx/hypopharynx are involved (the AJCC/TNM nomenclature should be used)?
- Is the pre-epiglottic space invaded?
- Is the paraglottic space invaded? If yes, which sites precisely?
- Are laryngeal cartilages invaded? If yes, to what degree (inner cortex vs through outer cortex)?
- Is there invasion of other structures beyond the larynx/hypopharynx, for example, strap muscles, soft tissues of the neck, carotid arteries, prevertebral space, or esophagus?
- Are there unilateral/bilateral lymph node metastases? What levels are involved?

In addition, at the authors' institution, the reporting radiologists also indicate how confident they are with respect to involvement of the key anatomic areas mentioned earlier, in particular if there are technical issues impairing a confident interpretation of imaging findings. Furthermore, when certain key findings are reported, we indicate the series and image numbers and we provide appropriately annotated key images. This procedure is especially useful for follow-up examinations and for coherent evaluation at multidisciplinary tumor boards. It is equally important to stress the fact that lack of appropriate clinical history related to previous treatment and lack of images from previous radiological examinations can lead to diagnostic uncertainty and, therefore, only a close cooperation with the referring physicians will ultimately lead to a high-quality radiologic report.

SUMMARY

The advent of high-resolution surface coils combined with parallel imaging techniques, more robust DWI techniques, and refined diagnostic criteria have been some of the most significant advances in oncologic imaging of the larynx and hypopharynx. Although MR imaging of the larynx and hypopharynx presents some technical challenges, advantages over CT outweigh disadvantages. Current state-of-the-art MR imaging allows a more precise assessment of submucosal tumor spread by detecting subtle soft-tissue abnormalities in anatomic areas that are more difficult to interpret on CT scans, such as the paraglottic space, the laryngeal cartilages, and the extralaryngeal soft tissues. Current MR imaging diagnostic criteria combining distinct signal intensity patterns on morphologic sequences with DWI features allow an improved discrimination between tumor, peritumoral inflammation and scar tissue, improved assessment of laryngeal cartilage abnormalities, and, ultimately, an increased precision for tumor delineation beyond the capability of multislice CT. Improved tumor delineation allows tailored treatment options, such as deciding between highly focused radiotherapy, transoral laser microsurgery, open partial laryngectomy, or total laryngectomy. Furthermore, MR imaging has a higher diagnostic performance than CT for the detection and precise depiction of post-treatment recurrent disease.

CLINICS CARE POINTS

- Both primary and recurrent laryngeal and hypopharyngeal SCCs have characteristic MR imaging features, which include an intermediate signal intensity on T1, T2, and T2 STIR, moderate contrast enhancement after iv. administration of gadolinium chelates and ADC values less than 1.3×10^{-3} mm^2/s
- Careful analysis of multiparametric MR imaging signal intensity allows distinction between tumor and peritumoral inflammation as inflammation has a higher signal intensity on T2 and T2 STIR and a stronger contrast enhancement than the tumor itself.[11,34,58] Also, on DWI, peritumoral inflammation shows no restriction of diffusion and ADC values are in general above 1.3×10^{-3} mm^2/s.
- Applying the current diagnostic MR imaging criteria for tumor, inflammation, normal nonossified and normal ossified cartilage, multiparametric MR imaging allows an improved diagnosis of cartilage abnormalities, thus avoiding diagnostic pitfalls related to CT.[11]
- The combination of morphologic MR imaging and DWI criteria allows improved detection of post-treatment recurrent disease and superior differentiation between residual tumor, late fibrosis, and post-treatment edema.[12,17,19] Although recurrent SCC has an intermediate T2 signal and low ADC values, late fibrosis/scar tissue is characterized by very low T2 signal and low ADC values. In contrast, post-treatment edema has high T2 signal and high ADC values.[12,17,19]

DISCLOSURE

The radiologic-pathologic correlation used to illustrate this article was part of a research project funded by the Swiss national Science Foundation (SNSF) under grant No 320030_173091/1.

REFERENCES

1. Nocini R, Molteni G, Mattiuzzi C, Lippi G. Updates on larynx cancer epidemiology. Chin J Cancer Res 2020;32(1):18–25.
2. Petersen JF, Timmermans AJ, van Dijk BAC, et al. Trends in treatment, incidence and survival of hypopharynx cancer: a 20-year population-based study in the Netherlands. Eur Arch Otorhinolaryngol 2018;275(1):181–9.
3. Bradley PJ. Epidemiology of hypopharyngeal cancer. Adv Otorhinolaryngol 2019;83:1–14.
4. Jones TM, De M, Foran B, et al. Laryngeal cancer: United Kingdom National Multidisciplinary guidelines. J Laryngol Otol 2016;130(S2):S75–82.
5. Gilbert K, Dalley RW, Maronian N, et al. Staging of laryngeal cancer using 64-channel multidetector row CT: comparison of standard neck CT with dedicated breath-maneuver laryngeal CT. AJNR Am J Neuroradiol 2009;31:251–6.
6. Becker M, Zbaren P, Delavelle J, et al. Neoplastic invasion of the laryngeal cartilage: reassessment of criteria for diagnosis at CT. Radiology 1997;203(2):521–32.
7. Becker M, Burkhardt K, Dulguerov P, et al. Imaging of the larynx and hypopharynx. Eur J Radiol 2008; 66(3):460–79.
8. Amin MB, Edge SB, Greene FL, et al, editors. AJCC cancer staging manual. 8th edition. New York: Springer-Verlag; 2017.
9. Brierley JD, Gospodarowicz MK, Wittekind C, editors. TNM classification of malignant tumours. Hoboken: Wiley Blackwell; 2017.
10. Becker M, Zbaren P, Laeng H, et al. Neoplastic invasion of the laryngeal cartilage: comparison of MR imaging and CT with histopathologic correlation. Radiology 1995;194(3):661–9.
11. Becker M, Zbaren P, Casselman JW, et al. Neoplastic invasion of laryngeal cartilage: reassessment of criteria for diagnosis at MR imaging. Radiology 2008;249(2):551–9.
12. Ravanelli M, Farina D, Rizzardi P, et al. MR with surface coils in the follow-up after endoscopic laser resection for glottic squamous cell carcinoma: feasibility and diagnostic accuracy. Neuroradiology 2013;55:225–32.
13. Preda L, Conte G, Bonello L, et al. Diagnostic accuracy of surface coil MRI in assessing cartilaginous invasion in laryngeal tumours: do we need contrast-agent administration? Eur Radiol 2017; 27(11):4690–8.
14. Vandecaveye V, De Keyzer F, Nuyts S, et al. Detection of head and neck squamous cell carcinoma with diffusion weighted MRI after (chemo)radiotherapy: correlation between radiologic and histo- pathologic findings. Int J Radiat Oncol Biol Phys 2007;67: 960–71.
15. Abdel Razek AA, Kandeel AY, Soliman N, et al. Role of diffusion- weighted echo-planar MR imaging in differentiation of residual or recurrent head and neck tumors and posttreatment changes. AJNR Am J Neuroradiol 2007;28:1146–52.
16. Thoeny HC, De Keyzer F, King AD. Diffusion-weighted MR imaging in the head and neck. Radiology 2012;263:19–32.
17. Varoquaux A, Rager O, Dulguerov P, et al. Diffusion-weighted and PET/MR imaging after radiation therapy for malignant head and neck tumors. Radiographics 2015;35(5):1502–27.
18. Becker M, Varoquaux AD, Combescure C, et al. Local recurrence of squamous cell carcinoma of the head and neck after radiochemotherapy: diagnostic performance of FDG-PET/MRI with diffusion weighted sequences. Eur Radiol 2018;28(2): 651–63.
19. Ailianou A, Mundada P, de Perrot T, et al. MRI with diffusion weighted imaging for the detection of post-treatment head and neck squamous cell carcinoma: why morphological MRI criteria matter. Am J Neuroradiol AJNR 2018. https://doi.org/10.3174/ajnr.A5548.
20. Casselman JW. High resolution imaging of the skull base and larynx. In: Schoenberg SO, Dietrich O, Reiser MF, editors. Parallel imaging in clinical MR applications. Berlin, Heidelberg, New York: Springer Science & Business Media; 2007. p. 199–208.
21. Ljumanovic R, Langendijk JA, van Wattingen M, et al. MR imaging predictors of local control of glottic squamous cell carcinoma treated with radiation alone. Radiology 2007;244:205–12.
22. Verduijn GM, Bartels LW, Raaijmakers CP, Terhaard CH, Pameijer FA, van den Berg CA. Magnetic resonance imaging protocol optimization for delineation of gross tumor volume in hypopharyngeal and laryngeal tumors. Int J Radiat Oncol Biol Phys 2009;74(2):630–6.
23. Maroldi R, Ravanelli M, Farina D. Magnetic resonance for laryngeal cancer. Curr Opin Otolaryngol Head Neck Surg 2014;22(2):131–9.
24. Ruytenberg T, Verbist BM, Vonk-Van Oosten J, et al. Improvements in high resolution laryngeal Magnetic Resonance Imaging for preoperative transoral laser microsurgery and radiotherapy considerations in early lesions. Front Oncol 2018;8:216. https://doi.org/10.3389/fonc.2018.00216.
25. Hermans R, Van den Bogaert W, Rijnders A, et al. Predicting the local outcome of glottic squamous cell carcinoma after definitive radiation therapy:

value of computed tomography-determined tumour parameters. Radiother Oncol 1999;50(1):39–46.
26. Dagan R, Morris CG, Bennett JA, Mancuso AA, Amdur RJ, Hinerman RW, Mendenhall WM. Prognostic significance of paraglottic space invasion in T2N0 glottic carcinoma. Am J Clin Oncol 2007; 30(2):186–90.
27. Lee JH, Machtay M, McKenna MG, et al. Radiotherapy with 6-megavolt photons for early glottic carcinoma: potential impact of extension to the posterior vocal cord. Am J Otolaryngol 2001;22: 43–54.
28. Succo G, Crosetti E, Bertolin A, et al. Treatment for T3 to T4a la- ryngeal cancer by open partial horizontal laryngectomies: prognos- tic impact of different pathologic tumor subcategories. Head Neck 2018; 40:1897–908.
29. Lucioni M, Lionello M, Guida F, et al. The thyrocricoarytenoid space (TCAS): clinical and prognostic implications in laryngeal cancer. Acta Otorhinolaryngol Ital 2020;40(2):106–12.
30. Peretti G, Piazza C, Mora F, et al. Reasonable limits for transoral laser microsurgery in laryngeal cancer. Curr Opin Otolaryngol Head Neck Surg 2016;24(2): 135–9.
31. Reidenbach MM. The paraglottic space and transglottic cancer: anatomical considerations. Clin Anat 1996;9:244–51.
32. Reidenbach MM. Borders and topographic relationships of the paraglottic space. Eur Arch Otorhinolaryngol 1997;254:193–5.
33. Sato K. Spaces of the Larynx. In: Functional histoanatomy of the human larynx. Singapore: Springer; 2018. https://doi.org/10.1007/978-981-10-5586-7_20.
34. Ravanelli M, Paderno A, Del Bon F, et al. Prediction of posterior paraglottic space and cricoarytenoid unit involvement in endoscopically t3 glottic cancer with arytenoid fixation by magnetic resonance with surface coils. Cancers (Basel) 2019;11(1):67.
35. Benazzo M, Sovardi F, Preda L, et al. Imaging accuracy in preoperative staging of T3-T4 laryngeal cancers. Cancers (Basel) 2020;12(5):1074.
36. Joo YH, Park JO, Cho KJ, et al. Relationship between preepiglottic space invasion and lymphatic metastasis in supracricoid partial laryngectomy with cricohyoidopexy. Clin Exp Otorhinolaryngol 2014;7(3):205–9.
37. Suoglu Y, Guven M, Kiyak E, et al. Significance of pre-epiglottic space invasion in supracricoid partial laryngectomy with cricohyoidopexy. J Laryngol Otol 2008;122(6):623–7.
38. Lee WT, Rizzi M, Scharpf J, et al. Impact of preepiglottic space tumor involvement on concurrent chemoradiation therapy. Am J Otolaryngol 2010;31(3): 185–8.
39. Ljumanović R, Langendijk JA, Schenk B, et al. Supraglottic carcinoma treated with curative radiation therapy: identification of prognostic groups with MR imaging. Radiology 2004;232(2):440–8.
40. Smits HJG, Assili S, Kauw F, et al. Prognostic imaging variables for recurrent laryngeal and hypopharyngeal carcinoma treated with primary chemoradiotherapy: a systematic review and meta-analysis. Head Neck 2021;43(7):2202–15.
41. Obid R, Redlich M, Tomeh C. The treatment of laryngeal cancer. Oral Maxillofac Surg Clin North Am 2019;31(1):1–11.
42. Becker M, Leuchter I, Platon A, et al. Imaging of laryngeal trauma. Eur J Radiol 2014;83(1):142–54.
43. Hatley W, Samuel E, Evison G. The pattern of ossification in the laryngeal cartilages: a radiological study. Br J Radiol 1965;38:585–91.
44. Zan E, Yousem DM, Aygun N. Asymmetric mineralization of the arytenoid cartilages in patients without laryngeal cancer. AJNR Am J Neuroradiol 2011; 32(6):1113–8.
45. Bennett A, Carter RL, Stamford IF, et al. Prostaglandin-like material extracted from squamous cell carcinomas of the head and neck. Br J Cancer 1980;41:204–8.
46. Gallo A, Mocetti P, De Vincentiis M, et al. Neoplastic infiltration of laryngeal cartilages: histocytochemical study. Laryngoscope 1992;102:891–5.
47. Gregor RT, Hammond K. Framework invasion by laryngeal carcinoma. Am J Surg 1987;154:452–8.
48. Zbaren P, Nuyens M, Curschmann J, et al. Histologic characteristics and tumor spread of recurrent glottic carcinoma: analysis on whole-organ sections and comparison with tumor spread of primary glottic carcinomas. Head Neck 2007;29(1): 26–32.
49. Zbaren P, Christe A, Caversaccio MD, et al. Pretherapeutic staging of recurrent laryngeal carcinoma: clinical findings and imaging studies compared with histopathology. Otolaryngol Head Neck Surg 2007;137(3):487–91.
50. Zhang SC, Zhou SH, Shang DS, Bao YY, Ruan LX, Wu TT. The diagnostic role of diffusion-weighted magnetic resonance imaging in hypopharyngeal carcinoma. Oncol Lett 2018;15(4):5533–44.
51. Varoquaux A, Rager O, Lovblad KO, et al. Functional imaging of head and neck squamous cell carcinoma with diffusion-weighted MRI and FDG PET/CT: quantitative analysis of ADC and SUV. Eur J Nucl Med Mol Imaging 2013;40(6):842–52.
52. Driessen JP, Caldas-Magalhaes J, Janssen LM, et al. Diffusion-weighted MR imaging in laryngeal and hypopharyngeal carcinoma: association between apparent diffusion coefficient and histologic findings. Radiology 2014;272(2):456–63.
53. Loevner LA, Yousem DM, Montone KT, et al. Can radiologists accurately predict preepiglottic space invasion with MR imaging? AJR Am J Roentgenol 1997;169(6):1681–7.

54. Zbaren P, Becker M, Lang H. Staging of laryngeal cancer: endoscopy, computed tomography and magnetic resonance versus histopathology. Eur Arch Otorhinolaryngol 1997;254(Suppl 1):S117–22.
55. Zbären P, Becker M, Laeng H. Pretherapeutic staging of hypopharyngeal carcinoma: clinical findings, computed tomography, and magnetic resonance imaging compared with histopathologic evaluation. Arch Otolaryngol Head Neck Surg 1997;123: 908–13.
56. Banko B, Djukic V, Milovanovic J, Kovac J, Novakovic Z, Maksimovic R. MRI in evaluation of neoplastic invasion into preepiglottic and paraglottic space. Auris Nasus Larynx 2014;41(5):471–4.
57. van Egmond SL, Stegeman I, Pameijer FA, et al. Systematic review of the diagnostic value of magnetic resonance imaging for early glottic carcinoma. Laryngoscope Investig Otolaryngol 2018;3(1): 49–55.
58. Allegra E, Ferrise P, Trapasso S, et al. Early glottic cancer: role of MRI in the preoperative staging. Biomed Res Int 2014;2014:890385. https://doi.org/10.1155/2014/890385.
59. Shang DS, Ruan LX, Zhou SH, et al. Differentiating laryngeal carcinomas from precursor lesions by diffusion-weighted magnetic resonance imaging at 3.0 T: a preliminary study. PLoS One 2013;8:e68622.
60. Beitler JJ, Muller S, Grist WJ, et al. Prognostic accuracy of computed tomography findings for patients with laryngeal cancer undergoing laryngectomy. J Clin Oncol 2010;28:2318–22.
61. Li B, Bobinski M, Gandour-Edwards R, et al. Overstaging of cartilage invasion by multidetector CT scan for laryngeal cancer and its potential effect on the use of organ preservation with chemoradiation. Br J Radiol 2011;84(997):64–9.
62. Li P, Hu W, Zhu Y, Liu J. Treatment and predictive factors in patients with recurrent laryngeal carcinoma: a retrospective study. Oncol Lett 2015; 10(5):3145–52.
63. Induction chemotherapy plus radiation compared with surgery plus radiation in patients with advanced laryngeal cancer. The department of veterans affairs laryngeal cancer study group. N Engl J Med 1991; 324:1685–90.
64. Tsai YT, Chen WC, Chien CY, et al. Treatment patterns and survival outcomes of advanced hypopharyngeal squamous cell carcinoma. World J Surg Oncol 2020;18:82. https://doi.org/10.1186/s12957-020-01866-z.
65. Becker M, Schroth G, Zbären P, et al. Long-term changes induced by high-dose irradiation of the head and neck region: imaging findings. Radiographics 1997;17(1):5–26.
66. Vaid S, Chandorkar A, Atre A, et al. Differentiating recurrent tumours from post-treatment changes in head and neck cancers: does diffusion-weighted MRI solve the eternal dilemma? Clin Radiol 2017; 72:74–83.
67. Tshering Vogel DW, Zbaeren P, Geretschlaeger A, et al. Diffusion-weighted MR imaging including bi-exponential fitting for the detection of recurrent or residual tumour after (chemo)radiotherapy for laryngeal and hypopharyngeal cancers. Eur Radiol 2013;23: 562–9.
68. Becker M, Moulin G, Kurt AM, et al. Non-squamous cell neoplasms of the larynx: radiologic-pathologic correlation. Radiographics 1998;18(5):1189–209.